Excitons and a Charge-Separated Pair in Thin Crystals of Oxotitanium(IV) Phthalocyanine As Revealed by Femtosecond Time-Resolved Absorption and Time-Correlated Single Photon Counting

Minoru Tsushima, Yoshiaki Motojima, Noriaki Ikeda, Hisatomo Yonehara,† Hideki Etori,† Chyongjin Pac,† and Takeshi Ohno*

Department of Chemistry, Graduate School of Science, Osaka University, 1−16 Machikaneyama, Toyonaka, Osaka 560-0043, Japan

Received: July 6, 2001; In Final Form: October 15, 2001

A photochemical study was performed by means of femtosecond time-resolved absorption spectroscopy on novel polymorphs of thin crystalline oxotitanium(IV) phthalocyanine $(OTiPc)_n$ ($n = 2-4$), β-OTiPc-L (phase I) and α-OTiPc-S (phase II), where the letters "L" and "S" mean "lying" molecular orientation and "standing" molecular orientation, respectively. A rapid change of the well time-resolved absorption spectrum in a range of 420−620 nm revealed that a part of the intrinsic exciton of β-OTiPc-L with the absorption maximum around 550 nm was in a lifetime of 0.5 ps converted to a charge-separated pair on the excitation of the 400 and 800 nm laser. The absorption bands at 430, 510, and ∼860 nm were left for a lifetime of 3 ps. The formation of the cationic π-radical inferred to be $^2(OTiPc)_{n-1}^+$ is responsible for the absorption bands at 510 nm and that of the anionic species of $^2(OTi^{III}Pc)^-$ is responsible for the band at 430 nm instead of the characteristic bands of the anionic π-radical of metallophthlocyanine around 600 nm. While the charge-separated pair disappeared in 10 ps, another transient absorption at 490 nm was survived on the excitation of the 400 nm laser, which is assigned to the triplet exciton formed via intersystem crossing from higher state(s) of the singlet exciton. The time-correlated single photon counting technique revealed that a novel fluorescence of α-OTiPc-S with a peak at 10 420 cm^{-1} decaying biexponentially with a short (48−64 ps) lifetime and a long (101−416 ps) lifetime is assigned to the trapped excitons. A 10-fold increase in the initial intensity of the fluorescence at 77 K compared with at 298 K indicates that the yield of long-lived and fluorescent exciton is smaller than 0.1 on the excitation of α-OTiPc-S at 298 K.

1. Introduction

Thin crystal of oxotitanium(IV) phthalocyanine (OTiPc) is one of the most efficient photoconductive materials.[1] Crystalline forms of OTiPc are chemically stable and display a strong and wide absorption band in a visible region. The primary process of photoinduced current generation has been rarely studied because the excited state involved in the charge separation could be so short-lived on account of the extremely high efficiency of photon-to-current conversion.[2] More recently, the biexponential decay of a fluorescence in 300 ps for the Y-form of crystalline OTiPc was examined under the electric field.[1−3] The field dependence of the initial amplitude and lifetime of the fast decay component suggested that intrinsic excitons with a charge-transfer character undergoing the carrier generation are converted to another mobile exciton with a short life (35 ps) of the fluorescence.[1] The long-lived (<200 ps) component of fluorescence was ascribed to a long-lived and trapped exciton, which originated from the mobile intrinsic exciton. A similar effect of the electric field on the short-lived fluorescence was observed for the Y-form of OTiPc most recently,[2,3] while no effect on the initial amplitude of short-lived fluorescence was observed for a less active crystalline form of OTiPc (phase I). The electric field effect on the intrinsic exciton is fitted with the assignments of excited states as either the neutral or charge-transfer state based on the Stark spectroscopy.[4] Charge separation and charge recombination on the photoexcitation of the ground-state charge-transfer complexes have been extensively studied in dilute solution[5,6] and neat solid.[7] The ultrafast processes of charge separation and charge recombination in a solid film of π-conjugated organic compound, α-sexithienyl, have been rarely investigated by means of time-resolved absorption spectroscopy.[8]

Meanwhile, a study of femtosecond time-resolved absorption spectroscopy on the Y-form of OTiPc revealed that excitons on the higher energy laser excitation of the OTiPc (Y-form) disappeared via annihilation within a couple of picoseconds to reduce the photoelectric response.[9] A kind of nonrelaxed exciton with a lifetime of 1 ps was considered as a possible precursor of charge-separated species. Such a nonrelaxed exciton was observed for OVPc by means of femtosecond time-resolved absorption spectroscopy, too.[10,11]

The present authors[12] succeeded in the preparation of several polymorphs of OTiPc by vacuum sublimation to a thin metal-on-glass. One of the polymorphs, α-form (phase II), which displays an absorption peak at the lowest energy due to the extent of molecular interaction among the polymorphs including the Y-form, exhibits a novel fluorescence with a lifetime of 50 ps in a near infrared region.[12] The temperature-dependence of the fluorescence quantum yield was investigated to find a short-lived precursor of charge-separated species by using the time-correlated single photon counting technique. Femtosecond time-resolved absorption spectroscopy was applied to both α-OTiPc-S (phase II) and β-form OTiPc-L (phase I) in order to look at the rise and decays of charge-separated pair and the recovery of the ground-state population.

† Kawamura Institute of Chemical Research, 631 Sakado, Sakura, Chiba 285-0078, Japan.

* Fax number: +81−6−6850−5785, E-mail address: ohno@ch.wani.osaka-u.ac.jp.

10.1021/jp0125597 CCC: $22.00
Published on Web 01/09/2002

2. Experimental Section

Preparation of Thin Crystals of OTiPc. OTiPc was synthesized according to a method developed by one of present authors and then purified by repeated vacuum sublimation under an argon flow.[12,13] Semitransparent metal-on-glass were obtained by evaporating Au on 1 mm thick Corning 7059 glass plates (20×20 mm^2) at 0.2 mm/s under $1 \times 10^{-3}-10^{-5}$ Pa and by sputtering Pt onto the glass plate at 0.1 nm/s. The thickness of metal was 20 nm. Polymorphs of OTiPc crystal were prepared on various metals by means of sublimation under 10^{-6} Pa at various temperatures with a depositing rate of 0.05 nm/s. The α-form crystal of 150−200 nm thickness in which OTiPc molecules are aligned with the molecular plane "standing" with respect to the substrate surface (α-OTiPc-S), was prepared on Pt at 150 °C under $10^{-3} \sim 4 \times 10^{-4}$ Pa. The α-form of 400 nm thickness in which OTiPc molecules are aligned with the molecular plane "lying" with respect to the substrate surface (α-OTiPc-L), were formed on Pt metal at 150 °C under 2.7×10^{-5} Pa. The *β*-form of 100 nm thickness with lying orientation of the molecular plane with respect to the substrate surface (*β*-OTiPc-L) was formed on Au at 150 °C. The α-form and *β*-form of the thin crystal are referred to the X-ray diffraction pattern of phase I and phase II, respectively.[12,14,15]

Spectra and Yield of Emission. The absorption spectra of the crystal samples were recorded by using JASCO V-570 spectrophotometer. The emission spectra were measured by using a grating monochromator (JASCO CT250) with a silicon diode array (Hamamatsu S3901−512Q). The sensitivity of the emission spectrometer was corrected by using a bromine lamp, Ushio JPD100V500WCS. The 514.5 nm line and 351 nm line of an Ar laser (Coherent Innova 306) were used for the excitation of the crystalline and the solution samples, respectively. For the measurement of fluorescence quantum yield (Φ) of α-OTiPc-S, $Ru(bpy)_3^{2+}$ in acetonitrile was used for a reference ($\Phi = 0.062$). A sample solution of OTiPc was prepared by dissolving a piece of the crystal in CH_2Cl_2 and then deaerated by bubbling Ar.

Decay of Emission. A time-correlated single-photon counting system with a cavity-dumped Ti^{3+}:Sapphire laser (100 fs, 20 nJ/pulse, and 380 kHz)[16] was used for the measurement of fluorescence decay. The fundamental pulse of the laser (760−840 nm) was used for generating a starting pulse from a PIN photodetector with 40 ps time constant (Hamamatsu C4258) and for the excitation of sample crystals. Quanta of the emission were detected by using a interference-filter ($T = 50\%$ max at 855, 905, or 940 nm and fwhm=10 nm) with a microchannel-plate photomultiplier (Hamamatsu R3809U-51X) that is cooled. The instrumental response function (IRF) of the detection system was determined by monitoring scattered quanta of the excitation laser from the sample. The full width at the half-maximum of IRF is typically 40 ps. The decays of emission were convoluted by using the IRF. Sample films on metal-on-glass were retained in a cryostat (Oxford Optistat DN1740) controlled by an Oxford ITC601 controller in the temperature range 77−298 K.

Femtosecond Time-Resolved Absorption Spectroscopy. Laser pulses with a repetition rate of 200 Hz were generated by a Ti^{3+}:sapphire based oscillator and a regenerative amplifier (Tsunami and Spitfire, Spectra Physics, Inc.). The width of the amplified laser was 200 fs with a wavelength centered at 800 nm and energy of 0.4 mJ. The fundamental pulse was frequency doubled by using a 1 mm BBO crystal to give a 400 nm pulse, which was used to excite the sample. The remainder of the fundamental pulse was focused into a 8 mm flow cell containing water, thereby generating a white light continuum. A polarizer was used to attain a linear polarization of the probe light and to rotate the polarization to 54.7° (magic angle) relative to that of the pump beam. Before passing through a sample, the probe beam was divided into a signal and reference beam by a 3 mm beam splitter inserted at 45°. The typical energy of the pump pulse was 25 *μ*J/pulse with the diameter of 1 mm at the sample. The signal beam through a sample and the reference beam were detected by a couple of image sensors (Hamamatsu S4805-512) attached to polychromators (Chromex 250IS). The full width at the half-maximum of the instrumental response function (IRF) was 300 fs. The arrival time of a white light continuum at the sample is dependent of the wavelength due to the group velocity dispersion. For this correction, the rise curve of the excited-state absorption of $Ru(bpy)_3^{2+}$ in CH_3CN was measured at various wavelengthes, of which the build-up time is within 100 fs.

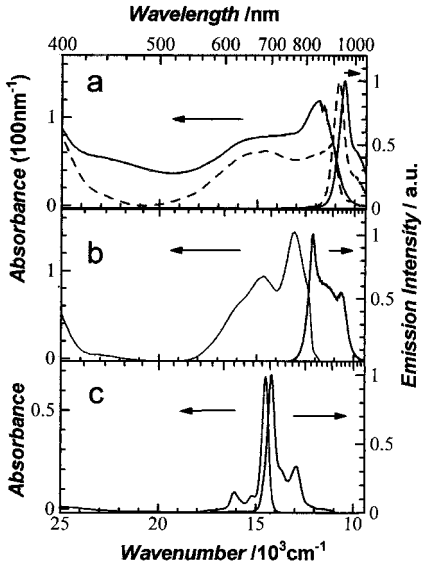

Figure 1. Absorption and fluorescence spectra at ambient temperature: (a) α-OTiPc-S (solid line) and α-OTiPc-L (dashed line); (b) *β*-OTiPc-; (c) the CH_2Cl_2 solution.

TABLE 1: Energies of Optical Transitions and Yield and Lifetime of Fluorescence for the Crystalline Samples and the CH_2Cl_2 Solution at 296 K

samples	α-OTiPc-S	α-OTiPc-L	*β*-OTiPc-L	CH_2Cl_2
lowest absorption peak /cm^{-1}	11 630	11 100	13 160	14 510
emission peak /cm^{-1}	10 420[a]	10 750	10 400 11 900	14 230
yield of emission	0.0036, 0.022,[a] 0.002[b]	-	0.0042	0.20
lifetime of emission /ps	53,[c] 100[d] 53,[a] 416[b]	-	21,[e] 58[f]	4000

[a] The short-lived component at 77 K. [b] The long-lived component at 77 K. [c] The short-lived component at 298 K. [d] The long-lived component at 298 K. [e] Fluorescence at 10 600 cm^{-1}. [f] Fluorescence at 11 700 cm^{-1}.

3. Results

3.1. Absorption and Fluorescence Spectra. A sharp and strong absorption band of OTiPc at 14 510 cm^{-1} in the CH_2Cl_2 solution is considerably broadened and shifted to lower energy in the crystalline OTiPc, α-OTiPc-S (11 630 cm^{-1}), α-OTiPc-L (11 100 cm^{-1}), and *β*-OTiPc-L (13 160 cm^{-1}), as Figure 1 and Table 1 show. The α-form of the OTiPC crystal emits a fluorescence at 10 420 cm^{-1} for α-OTiPc⊥ and 10 750 cm^{-1} for α-OTiPc-L, which are lower in energy by more than 3500 cm^{-1} than in a solution. A width of the fluorescence band (700

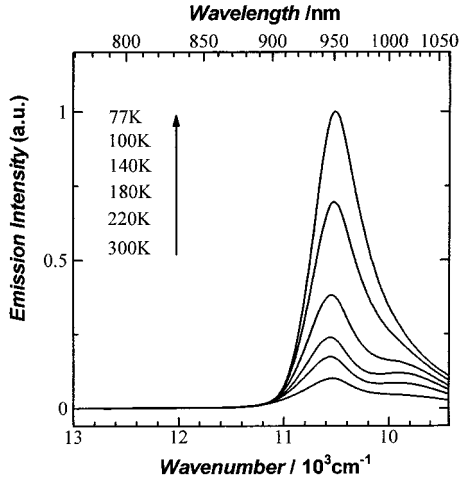

Figure 2. Temperature-dependent fluorescence of α-OTiPc-S in a range of 77−300 K.

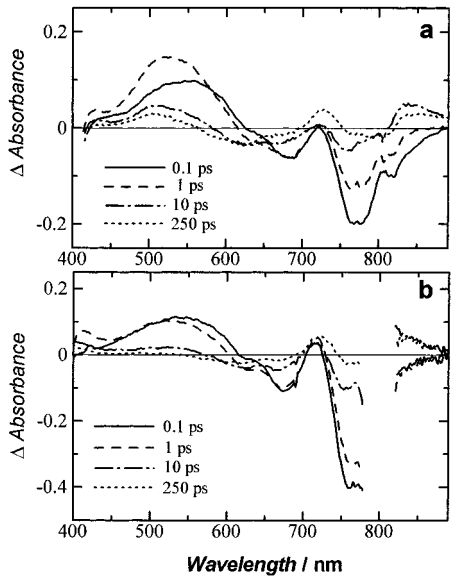

Figure 3. Time-resolved difference absorption spectra of β-OTiPc-L on the 400 nm laser excitation (a) and on the 800 nm laser excitation (b). The delay times are shown after the laser excitaiton.

cm^{-1}) of the α-form larger than 400 cm^{-1} in the solution suggests the presence of various dipole−dipole interactions due to the imperfect structure of the crystal.[12] The spectra are almost independent of temperature, as is shown in Figure 2. The fluorescence of the α-form is different from those reported of the Y-form; the peak energies (10 420 cm^{-1} for α-OTiPc-S and 10 750 cm^{-1} for α-OTiPc-L) are much lower than 11 760 cm^{-1} of the Y-form.[1,9] The crystal of β-OTiPc-L emits a higher energy fluorescence with a maximum at 11 900 cm^{-1} in addition to that at 10 420 cm^{-1}, as Figure 1b shows.

3.2. Time-Resolved Absorption Spectra and Its Time Profile of β-OTiPc-L. Time-resolved absorption spectra of β-OTiPc-L at various delay times from the excitation of the 400 or 800 nm laser exhibited the bleaching of the ground-state absorption (negative absorbance) in a wide range of 600−890 nm and the formation of an absorption (positive absorbance) in the range 420−620 nm, as are shown in Figure 3. The difference absorption spectra contain scattered intensities around the excitation wavelengths, 400 and 800 nm. The amount of the bleached absorption at 755 nm immediately after the laser excitation is linear to the laser intensity, as is shown in Figure 4.

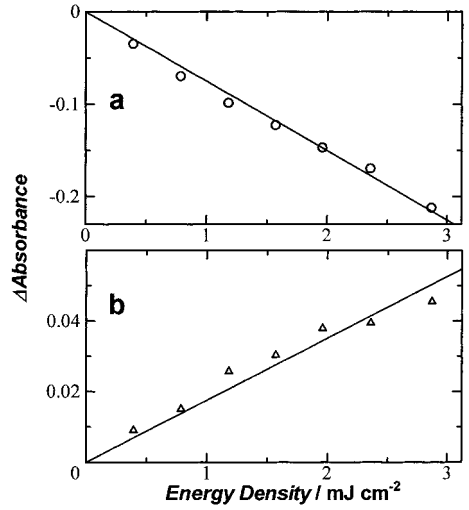

Figure 4. Relation between the difference absorption of β-OTiPc-L and the laser intensity for the excitation: (a) production of difference absorption at 750 nm immediately after the laser excitation; (b) difference absorption at 570 nm left at 3 ps after the laser excitation.

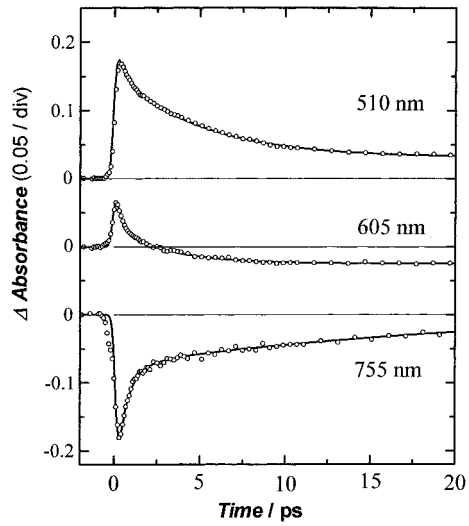

Figure 5. Time profiles of the difference absorption of β-OTiPc-L at 510, 605, and 755 nm at 296 K: (○) observed; (solid lines) fitting function of difference absorption, $\Delta A(t) = \sum \Delta A_i \exp(-k_i t)$.

The peak of the difference absorption band was shifted from 550 to 510 nm and new peaks at 730 and 850 nm emerged for 2 ps. During this spectral shift, both the bleached absorption at 755 nm on the 400 nm excitation and at 746 nm on the 800 nm excitation were reduced to 31% of the initial one. The difference spectrum at 250 ps exhibits a broad band with peaks at 420 and 510 nm, and a zigzag band in a wavelength region longer than 600 nm with positive peaks at 730 and 850 nm and with negative peaks at 620 and 780 nm.

Decays of the difference absorptions of β-OTiPc-L at 510, 605, and 755 nm were multiexponential on the 400 nm excitation, as are shown in Figure 5. The fast component of decay and the slow one of the absorption band at 510 and 605 nm were 17×10^{11} and 2.0×10^{11} s^{-1}, respectively. The first and the second recoveries of the ground-state-absorption at 755 nm occurred with a rate constant of 23×10^{11} and 3.8×10^{11} s^{-1}, while the third recovery was much slower (0.41×10^{11} s^{-1}). A total of 68% of the bleached ground-state absorption was recovered within 10 ps and the rest (32%) was recovered then. The difference absorption in a range of 450−620 nm decayed more slowly than the major recovery of the bleached

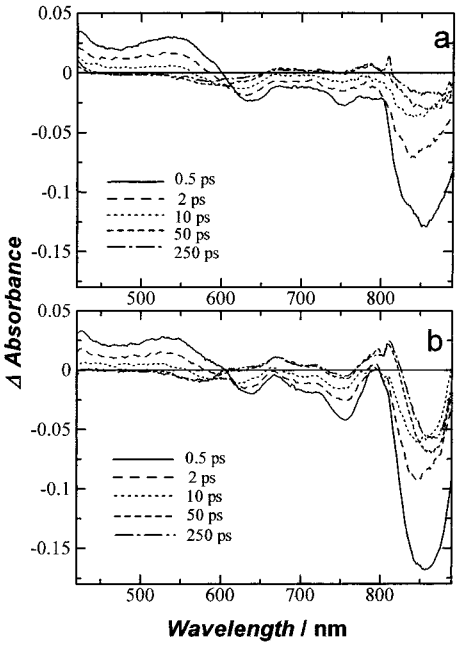

Figure 6. Time-resolved difference absorption spectra of α-OTiPc-S (a) at 296 K and (b) at 77 K. The delay times are shown after the laser excitation.

absorbance. The absorption left at 3 ps after the laser excitation (ΔA_{570}) was linear to the laser intensity.

3.3. Time-Resolved Absorption Spectra and Its Time Profile of α-OTiPc-S. Time-resolved difference spectra of α-OTiPc-S immediately after the laser excitation consist of broad bands with two peaks at 430 and 540 nm and bleached bands at 630, 750, and 860 nm, as is shown in Figure 6. The difference absorption spectrum after 2 ps became more similar to that of *β*-OTiPc-L with an exception of the bleached band at 860 nm. A peak of the bleached band at 860 nm was shifted to 840 nm in 2 ps, followed by a return to 860 nm in a time course of 10−50 ps. The difference absorption spectrum at 250 ps delay consists of small negative and positive peaks in a red region.

Decays of the difference absorption bands of α-OTiPc-S at various wavelengths were not single exponential, as are shown in Figure 7. The recovery of the bleached ground-state absorption at 755 nm occurred in three steps; the first one with a rate constant of 35×10^{11} s^{-1}, the second one with a rate constant of 5.4×10^{11} s^{-1}, and the third one with a rate-constant of 0.41×10^{11} s^{-1} at 296 K. Lowering the temperature increased the rate of the second process. The first decay component of the difference absorption at 510 nm was small, while the second and the last components of decay occurred with rate constants similar to those of the recovery process monitored at 751 nm. The intensity of the excitation laser had a weak influence on the fast recovery of ground-state absorption, as Figure 8 shows. A total of 76% of the bleached one was recovered within 5 ps and 24% was recovered within 100 ps at 296 K.

3.4. Yields and Decays of Long-Lived Fluorescence. The decay of the fluorescence intensity shown in Figure 9 is written by using two exponential terms,

$$I(t) = I_S \exp(-t/\tau_S) + I_L \exp(-t/\tau_L) \quad (1)$$

where I_S and I_L are the initial intensity of the short-lived decay component and the long-lived decay component, respectively, and τ_S and τ_L are the lifetime of the short-lived component and the long-lived component, respectively. τ_S is 35−70 ps irrespective of temperature, while τ_L increases from 100 ps at 296 K to

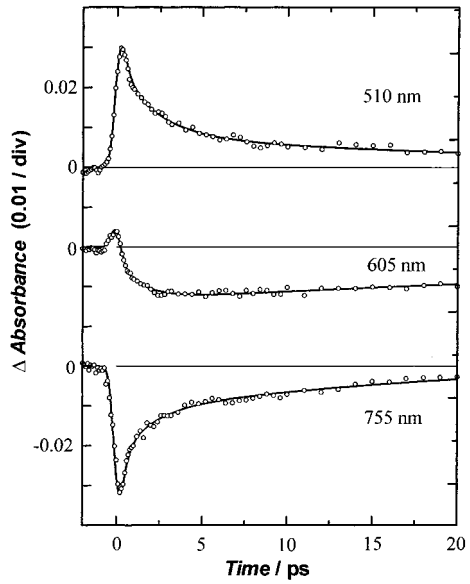

Figure 7. Time profiles of the difference absorption of α-OTiPc-S at 510, 605, and 755 nm at 296 K: (○) observed; (solid line) fitting function of difference absorption is $\Delta A(t) = \sum \Delta A_i \exp(-k_i t)$.

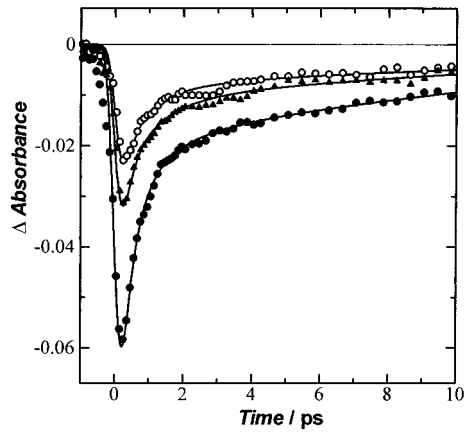

Figure 8. Dependence of the recoveries observed and calculated of the ground-state absorption at 751 nm on the intensity of laser for the excitation of α-OTiPc-S. (○), (▲), and (●) represent the recovery observed on the laser excitation of the 1.1, 1.5, and 3.1 mJ/pulse, respectively. The solid lines are calculated by using the fitting rate constants of $\Delta A(t) = \sum \Delta A_i \exp(-k_i t)$, (28, 9.2, and 0.53) $\times 10^{11}$ s^{-1} on the 1.1 mJ laser ecitation, (37, 9.4, and 0.60) $\times 10^{11}$ s^{-1}on the 1.5 mJ laser excitation and (33, 11, and 0.58) $\times 10^{11}$ s^{-1} on the 3.1 mJ laser excitation, respectively.

416 ps at 77 K with a decrease in the temperature, as is shown in Figure 10.

The yields of fluorescence at 296 K were as low as 0.0036 and 0.0042 for α-OTiPc-S and *β*-OTiPc-L, respectively. The fluorescence yield of α-OTiPc-S was dependent on temperature. The fluorescence yield of the α-form (α-OTiPc-S) increased from 0.0025 at 260 K to 0.023 at 77 K, which is still smaller than that (0.2) of OTiPc dissolved in CH_2Cl_2 at 296 K. The initial intensity of the short-lived component increases with a decrease in temperature from 0.45×10^8 at 260 K to 4.42×10^8 at 77 K, while that of the long-lived component remains nearly constant throughout the temperature range, as is shown in Table 4 and Figure 11.

4. Discussion

4.1. Reactions of Intrinsic Exciton and Charge-Separated Pair in *β*-OTiPc L. The formation of photoproduct with a short

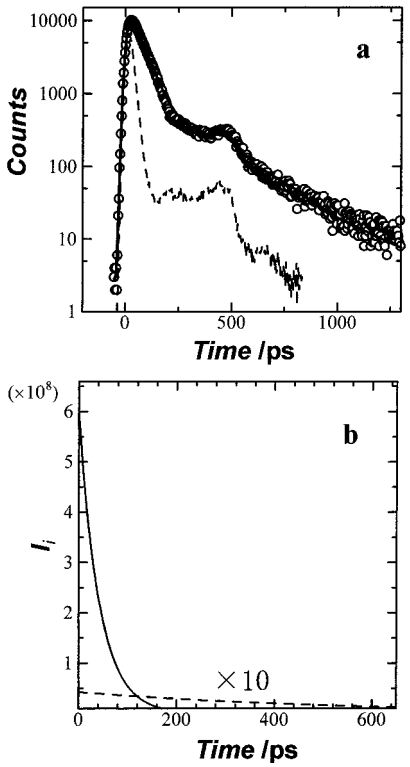

Figure 9. Time profile of fluorescence of α-OTiPc-S at 77 K and the instrument response function: (a) observed decay (open circles) and simulated line (solid line) convoluted by using the IRF (dotted line); (b) decay of short-lived component (solid line) and decay of long-lived component (dashed lined).

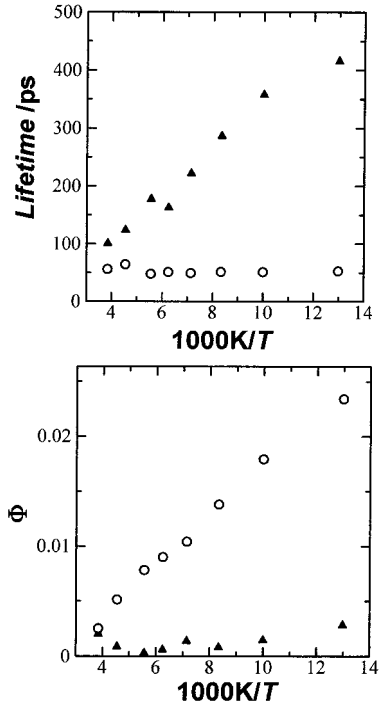

Figure 10. Temperature dependence of lifetimes (top) and quantum yields (bottom) of the short-lived component (○) and long-lived component (▲) of fluorescence.

life of 0.3−0.5 ps was observed as a time-resolved difference absorption spectrum immediately after the laser excitation. The difference absorption spectrum of the major photoproduct with the peak at 560 nm is similar to that of the singlet excited state of metallophthalocyanine in solution[18] and of the short-lived

TABLE 2: Rate Constants (k_1, k_2, and k_3) and Amplitudes (ΔA_1, ΔA_2, and ΔA_3) of the Difference Absorption Observed at Various Wavelengths after the Excitation of β-OTiPc-L at 296 K[a]

wavelength/nm	ΔA_1	$k_1/10^{11}$ s^{-1}	ΔA_2	$k_2/10^{11}$ s^{-1}	ΔA_3	$k_3/10^{11}$ s^{-1}
510	0.032	17	0.124	2.0	0.032	
605	0.084	29	0.054	3.2	−0.024	
755	−0.17	23	−0.009	3.8	−0.085	0.41
850	−0.072	15	−0.066	2.0	−0.070	0.25

[a] The fitting function of difference absorption is $\Delta A(t) = \sum \Delta A_i \exp(-k_i t)$.

TABLE 3: Rate Constants (k_1, k_2, and k_3) and Amplitudes (ΔA_1, ΔA_2, and ΔA_3) of the Difference Absorption Observed at Various Wavelengths after the Excitation of α-OTiPc-S at 296 K[a]

wavelength/nm	ΔA_1	$k_1/10^{11}$ s^{-1}	ΔA_2	$k_2/10^{11}$ s^{-1}	ΔA_3	$k_3/10^{11}$ s^{-1}
510	0.027	31	0.018	4.5	0.008	0.38
605	0.031	53	0.009	5.9	−0.013	0.20
755	−0.037	35	−0.014	5.4	−0.014	0.41
850	−0.077	23	−0.084	5.5	−0.035	0.04

[a] The fitting function of difference absorption is $\Delta A(t) = \sum \Delta A_i \exp(-k_i t)$.

TABLE 4: Lifetimes (τ_s,τ_l), Quantum Yields (ϕ_s,ϕ_l), and Relative Formation Yields ($10^8(I_I^o/I_{abs})$, $10^8(I_{II}^o/I_{abs})$) of the Exciton-l and Exciton-s for α-OTiPc-S in the 77−298 K Region

T/K	τ_s/ps	τ_l/ps	ϕ_s	ϕ_l	$10^8(I_I^o/I_{abs})$	$10^8(I_{II}^o/I_{abs})$
298	50	370	0.0034	0.00017	0.692	0.0047
260	56	101	0.0025	0.00020	0.450	0.0200
220	64	124	0.0051	0.00087	0.802	0.0070
180	48	178	0.0078	0.00029	1.64	0.0166
160	51	163	0.0090	0.00060	1.76	0.0373
140	49	222	0.010	0.0014	2.13	0.0622
120	52	287	0.014	0.00081	2.68	0.0282
100	51	358	0.018	0.0015	3.52	0.0407
77	53	416	0.023	0.0028	6.86	0.0442

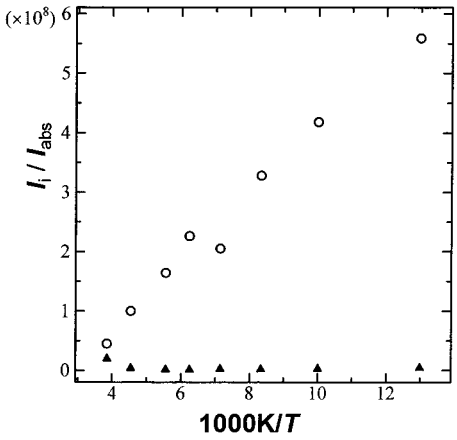

Figure 11. Temperature dependence of the normalized initial intensities (I_s/I_{abs} and I_l/I_{abs}) of the short-lived component (○) and long-lived component (▲) of fluorescence.

exciton of crystalline OVPc[9] and CuPc.[10] Therefore, the photoproduct may be a kind of singlet exciton.

The laser intensity was not large enough to pump all the ground-state molecules. The absorbance of the low-energy absorption band at 770 nm was reduced to 48% of the original one, while that of the high-energy absorption band at 650 nm was reduced to 74%. It is suggested that the singlet exciton exhibits an absorption band in the 600−720 nm region with a half-intensity of the ground-state absorption on the assumption that the exciton does no absorption at 770 nm. The formation

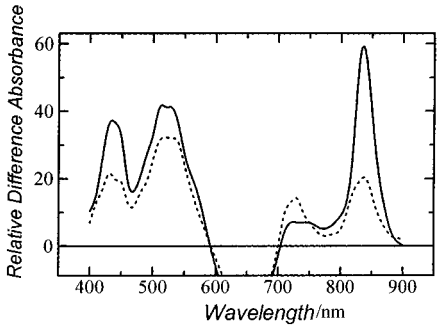

Figure 12. Transient difference absorption spectra on the laser excitation of 4 μM magnesium phthalocyanine (MgPc) in dimethylformamide containing of 800 μM $Co(bpy)_3^{3+}$. The solid line spectrum at 10 μs after the laser flashing was identified as $^2MgPc^+$, and the dashed line spectrum at 12 ms after the laser flashing was identified as $^2(MgPc)_2^+$.[20]

of photoproduct (2.2×10^{13} molecule/pulse) is estimated from the bleached absorption at 755 nm by using the molar extinction coefficient (57 000 mol^{-1} dm^3 cm^{-1}) on the laser excitation. The quantum yield of the exciton formation is calculated to be 0.9 by using the absorbed quanta of a laser pulse (3.2×10^{13}). The large yield of the bleaching (0.9) implies that the exciton does not escape from the measurement. A difference absorption band with a peak at 550 nm and a shoulder at 420 nm can be identified as the singlet exciton, too, because the intensity of the absorption band emerging without any delay is linear to the laser intensity as that of the bleached band at 755 nm. (Figure 4).

The difference absorption spectrum at 2 ps with a strong peak at 510 nm and two weak peaks around 420 and 850 nm in Figure 3 can be attributed to the formation of $^2(OTiPc)_{n-1}^+$ ($n = 2, 3, ...$) and $^2OTiPc^-$ by comparing with the absorption spectra of $^2(MPc)_2^+$ ($M = Mg^{2+}$ and Zn^{2+})[19,20] and $^2OTiPc^-$ in solution. As has been shown in Figure 12 by one of the present authors,[18−20] the absorption spectra of $^2(MPc)_2^+$ exhibited strong bands at 510 and 730 nm and weak bands at 420 and 840 nm in solution,[19,20] though those of MPc ($M = AlCl^{2+}$ and $InCl^{2+}$) exhibited similarly strong bands at 420, 510, and 840 nm in solution.[22] Another band at 730 nm might be hidden by the bleached ground-state absorption. Consequently, the distinct band at 510 nm in Figure 3 can be ascribed to the formation of $^2(OTiPc)_{n-1}^+$ ($n = 2, 3, ...$). The absorption spectrum of the reduced species, meanwhile, might resemble that of $^2OTiPc^-$, because any anionic π-radical never exerts dimerization in solution. The characteristic absorption peaks of the anionic π-radical of $^2MPc^-$ ($M = Mg^{2+}$, Zn^{2+}, Al^{3+}, Ni^{2+})[22,23] around 600 nm were not observed at all for the thin crystal of OTiPc exposed to the laser. To ascertain an absorption spectrum of a reduced species of OTiPc, spectroscopic work by using the third harmonics (355 nm) of a mode-locked Nd^{3+}:YAG laser was examined by photoexcitation of OTiPc in CH_2Cl_2 containing 1 M 1,2,4-trimethoxybenzene (TMB) and in 1-chloronaphthalene containing 1 M diphenylamine (DPA). Two bands at 430 and 460 nm appeared on the laser excitation, as is shown in Figure 13, of which the former is ascribed to not a π-radical of $^2OTi^{IV}$-Pc but $^2(OTi^{III}Pc)^-$ and the latter to $^2TMB^+$.[24,25] The band at 430 nm was also detected together with $^2DPA^+$, which displayed a broad band with the peak around 675 nm[26] (not presented). Consequently, the weak band on the photoexcitation of β-OTiPc-L around 430 nm might be attributed to the reduced oxotitanium-(III) group.

Judging from the rapid recovery of the ground-state absorption during the decay of the singlet exciton, the recovery of the

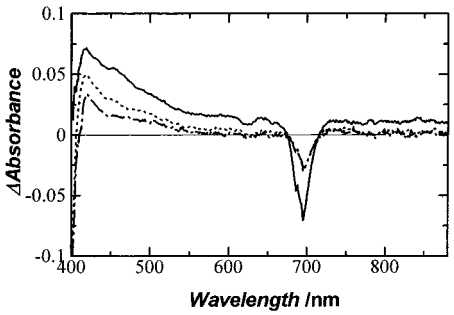

Figure 13. Time-resolved difference absorption spectra of OTiPc in CH_2Cl_2 containing 1 M 1,2,4-trimethoxybenzene on the 355 nm laser excitation: (solid line) 20 ps, (dotted line) 500 ps, and (dash−dot−dash line) 3000 ps after the laser excitaiton.

ground-state population occurred more efficiently than the formation of a charge-separated pair. The nascent exciton, $^1(OTiPc)_n$**, is considered to have a high reactivity of charge separation because of the rapid conversion to the charge-separated pair in a lifetime of 0.4 ps. Probably, the nascent excitons produce charge-separated pairs with various separation distances, of which shortly separated pairs, $^1[(OTiPc)_{n-1}^+ \cdot OTiPc^-]$, disappear in a very short time and long separated ones, $^2(OTiPc)_{n-1}^+ \cdots {}^2OTiPc^-$, exhibit a lifetime as long as 3 ps. The characteristics of the nascent exciton are absolutely different from that of the long-lived and fluorescent exciton. Since such a high reactivity of the nascent exciton was retained on the 800 nm laser excitation, the high reactivity could be characteristic of the nascent exciton. Such a reactive and short-lived exciton has been denoted as "an intrinsic exciton".[1]

The ground-state absorption at 755 nm was recovered in three steps, which are presumed as the following three processes,

$$^1(OTiPc)_n** \rightarrow {}^1[(OTiPc)_{n-1}^+ \cdot OTiPc^-] \rightarrow {}^1(OTiPc)_n*, \; {}^3(OTiPc)_n*, \text{ or } (OTiPc)_n \qquad k_1 \quad (2)$$

$$\rightarrow {}^2(OTiPc)_{n-1}^+ \cdots {}^2OTiPc^-$$

$$^2(OTiPc)_{n-1}^+ \cdots {}^2OTiPc^- \rightarrow (OTiPc)_n, \; {}^1(OTiPc)_n*, \text{ or } {}^3(OTiPc)_n* \qquad k_2 \quad (3)$$

$$^1(OTiPc)_n* \rightarrow (OTiPc)_n \qquad k_3 \quad (4)$$

where $^1(OTiPc)_n$**, $^1(OTiPc)_n$*, and $^3(OTiPc)_n$* are the nascent exciton, the long-lived and fluorescent exciton, and the triplet exciton, respectively. The first and second recovery of the bleached ground-state absorption at 755 nm ($\Delta A_{755}(t)$) was expressed by using the following equation,

$$\Delta A_{755}(t) = A_1 e^{-k_1 t} + A_2 e^{-k_2 t}$$

$$A_1 = \Delta\epsilon_G \Delta C_E^o + \Delta\epsilon_G f \Delta C_E^o \frac{k_1}{k_2 - k_1},$$

$$A_2 = -\Delta\epsilon_G f \Delta C_E^o \frac{k_1}{k_2 - k_1} \quad (5)$$

where $\Delta\epsilon_G$, ΔC_E^o, and f are the molar extinction coefficient change of exciton formation at 755 nm, the formation of the singlet exciton, and the fraction of $^2(OTiPc)_{n-1}^+ \cdots {}^2OTiPc^-$ formation in the decay of intrinsic exciton. The rate constants of k_1, k_2, and k_3 are 23×10^{11}, 3.8×10^{11}, and 0.41×10^{11} s^{-1}, respectively.

The decay of the intrinsic exciton and the rise and decay of $^2(\mathrm{OTiPc})_{n-1}^+$ are reflected on the time profile of absorption change at 510 nm ($\Delta A_{510}(t)$),

$$\Delta A_{510}(t) = A_1'\mathrm{e}^{-k_1 t} + A_2'\mathrm{e}^{-k_2 t}$$

$$A_1' = \Delta\epsilon_{\mathrm{E}}\Delta C_{\mathrm{E}}^{\mathrm{o}} + \Delta\epsilon_{\mathrm{h}} f \Delta C_{\mathrm{E}}^{\mathrm{o}} \frac{k_1}{k_2 - k_1},$$

$$A_2' = -\Delta\epsilon_{\mathrm{h}} f \Delta C_{\mathrm{E}}^{\mathrm{o}} \frac{k_1}{k_2 - k_1} \quad (6)$$

where $\Delta\epsilon_{\mathrm{E}}$ and $\Delta\epsilon_{\mathrm{h}}$ are the molar extinction coefficient change of exciton formation and $(\mathrm{OTiPc})_{n-1}^+$ formation, respectively. Only, the values of k_1 and k_2 were determined to be 17×10^{11} and 2.0×10^{11} s^{-1}, respectively. Since the fast decay is close to that (23×10^{11} s^{-1}) for the recovery of the ground-state absorption, it can be identified as the decay of the intrinsic exciton. The second decay at 510 nm is assumed to be the decay of the charge-separated pair, $^2(\mathrm{OTiPc})_{n-1}^+\cdots{}^2\mathrm{OTiPc}^-$.

If the annihilation reaction between intrinsic excitons was so rapid to compete with the formation of the charge-separated pair as in the case of OVPc,[10,11] the magnitude of ΔA_{570} at 3 ps, which is a measure of the formation of the charge-separated pair, would reach a plateau value with an increase in the laser energy. As Figure 4 shows, a linear relation between ΔA_{570} at 3 ps and the laser intensity confirms that a majority of the intrinsic exciton disappeared in its unimolecular decay, as shown in eq 2.

The time profile of the absorption at 850 nm was rather complex: the bleaching of the ground-state absorption was replaced through two steps of 0.5 ps lifetime and 5 ps lifetime by an absorption band of $^2\mathrm{OTiPc}^+$. A decay of the positive difference absorption at 850 nm can be ascribed to the decay of monomer radical, followed by a slow rise of a long-lived unknown species in 100 ps.

The absorption band left at 250 ps in the 420−550 nm region on the 400 nm excitation can be identified as the longer-lived triplet exciton, which is considered to exhibit such a broad absorption with the maximum at 490 nm as an isolated molecule in the excited triplet state in the solution[19,20,22] because triplet excited states of aromatic compounds exert a weak intermolecular interaction with the ground state.[27,28] Meanwhile, the absence of the difference absorption band at 250 ps on the 800 nm excitation indicates an efficient intersystem crossing to the triplet exciton occurs only from a somewhat higher energy level of the long-lived singlet exciton. No effect of the excitation wavelength on the intensity of the up-and-down difference band at 250 ps around 800 nm implies that the up-and-down difference band is not ascribed to the formation of triplet exciton. The origin of the up-and-down difference band will be ascribed to the thermal broadening of the structured spectrum given by the laser excitation in the following section.

4.2. Reactions of Intrinsic Exciton in α-OTiPc-S. The time-resolved absorption spectra in the 430−880 nm region was almost unchanged in shape, while the peak of the bleached absorption band in 800−880 nm was varied a little. The difference absorption spectra in the 420−650 nm region was rather similar to that of $^2(\mathrm{OTiPc})_{n-1}^+\cdots{}^2\mathrm{OTiPc}^-$ for β-OTiPc-L. The decays of the difference absorption at 510 and 605 nm and the recovery of the ground-state absorption occurred in two steps over 10 ps. The fastest and the second fastest recoveries of the ground-state absorption (35×10^{11} and 5.4×10^{11} s^{-1}) are attributed to the decays of the intrinsic exciton and the charge-separated pair, $^2(\mathrm{OTiPc})_{n-1}^+\cdots{}^2\mathrm{OTiPc}^-$, respectively.

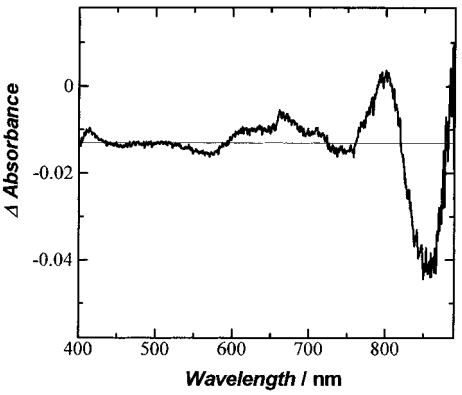

Figure 14. Absorption change induced by heating α-OTiPc-S from 77 to 127 K. A horizontal line might be the zero absorption line corrected by a difference absorption of the Pt plate of the photoirradiated thin crystal.

The decays of the difference absorption at 510 and 605 nm were also analyzed by using eq 3. The rate constant of the fastest decay at 510 nm (31×10^{11} s^{-1}) is close to k_1 of the first ground-state recovery at 755 nm and the fastest decay at 605 nm, while the second one at 510 nm is close to the second recovery of the ground-state population. The faster rates of the rise and the decay of $^2(\mathrm{OTiPc})_{n-1}^+\cdots{}^2\mathrm{OTiPc}^-$ compared with β-OTiPc-L (phase I) can be ascribed to the more extent of molecular interaction between OTiPc molecules in α-OTiPc-S (phase II). The slowest recovery (0.41×10^{11} s^{-1}) might occur from a long-lived and fluorescent exciton, as described in the following section.

The decay of intrinsic exciton within 1 ps was almost independent of the laser intensity for the excitation. Curve fitting of the fast recovery by using a common set of the rate constants was almost successful for all the recovery curves observed by using the various intensities of excitation laser, as shown in Figure 8. The participation of annihilation in the entire decay of intrinsic exciton could be minor. This is contrast to the observation that a rapid annihilation between intrisic excitons of the Y-form retards the charge separation on the laser excitation.[9]

A total of 76% of the bleached ground-state absorption was recovered within 10 ps and the 24% within 100 ps. The slowest recovery of the ground-state absorption might be related to the decay of long-lived excitons with a fluorescence lifetime of 53 ps.

An up-and-down difference spectrum was exhibited on heating the sample: a negative peak and a positive peak were produced for the peak and the valley of an original absorption band due to a thermal broadening of the band structure, respectively. Such a difference absorption spectrum at a long time delay was observed for the crystal of OVPc excited by using a high energy laser.[11] The higher extent of the bleached peak absorption at 864 nm as the temperature decreases (see Figure 14) can be accounted for by the increase in the absorption intensity due to the sharpening of absorption band with decrease in temperature.

4.3. Fluorescence of Long-Lived Exciton. A majority of the intrinsic exciton decayed in 2 ps to form the charge-separation products and other intermediates, of which the former also decayed within 10 ps. Decays of the long-lived excitons among other long-lived intermediates were examined by using a time-correlated single photon counting method. A fast communication between two excitons is not thought to occur during the lifetimes for the following reason. The short-lived (53 ps) exciton and the trapped and long-lived (416 ps) exciton

are designated "exciton-s" and "exciton-l" for convenience. The long-lived exciton-l is never the precursor of short-lived exciton-s. The exciton-s is not the precursor of exciton-l, because a 10-fold increase in the initial emission intensity of the exciton-s at 77 K was not accompanied by that of the long-lived component. The imperfect crystal structure of α-OTiPc-S allows the presence of the dual sites, though the thin crystal was well characterized by X-ray diffraction pattern.[12]

Since the fluorescence yield (Φ) is the sum of two fractions, which are the product of the formation yield of exciton-s or exciton-l (ϕ_S or ϕ_L) and the fraction of fluorescence in the decay of exciton-s or exciton-l (τ_S/τ_S^o or τ_L/τ_L^o), as is shown by

$$\Phi = \phi_S\left(\frac{\tau_S}{\tau_S^o}\right) + \phi_L\left(\frac{\tau_L}{\tau_L^o}\right) \tag{7}$$

the initial intensity and the lifetime of fluorescence were measured in order to find the major factor affecting the fluorescence yield, ϕ or τ/τ^o. When eq 7 is divided by the photon absorbed (I_{abs}) and is integrated over the time, the quantum yield of fluorescence is obtained,

$$\Phi = \left(\frac{I_S}{I_{abs}}\right)\tau_S + \left(\frac{I_L}{I_{abs}}\right)\tau_L \tag{8}$$

Though a ratio of the formation yield of exciton-s or exciton-l to the natural lifetime is determined from the relative intensity and the lifetime, each of the quantities is not determined separately.

The initial magnitude of the normalized intensity is a quantitative measure of the formation of exciton-s and exciton-l because relations $\phi_S/\tau_S^o = I_S/I_{abs}$ and $\phi_L/\tau_L^o = I_L/I_{abs}$ hold, provided that the natural lifetimes of exciton-s and exciton-l are the same. Since the initial intensity of the long-lived component is $^1/_{130}$th of the short-lived component at 77 K, the formation of exciton-l (ϕ_L) is much smaller than that of exciton-s. Consequently, the quantum yield of fluorescence from exciton-l is only 0.003 compared with that of the short-lived component (0.023) at 77 K even though the lifetime of exciton-l is much longer than that of exciton-s . In other words, the crystal sites for exciton-l are rare in α-OTiPc-S. Hence, the discussion will be focused on exciton-s hereafter.

The normalized fluorescence intensity from exciton-s ($I_S/I_{abs} = \phi_S k_r$) at 77 K increased to 10 times of that at 260 K, as is shown in Table 4. Though the magnitude of the radiative rate constant is unknown, the formation yield of the long-lived and fluorescent exciton-s (ϕ_S) at 298 K is less than 0.1 from the results of the temperature dependence. The small formation yield of exciton-s at 298 K implies that the intrinsic exciton exerts the charge separation mainly. The rate constants of the intrinsic exciton undergoing the charge separation and internal conversion are $k_{cs}(T)$ and k_{ic}, respectively, of which the former is dependent on temperature. The formation yield of exciton-s can be written in terms of the rate constants of intrinsic exciton,

$$\phi(T) = \frac{k_{ic}}{k_{ic} + k_{cs}(T)} \tag{9}$$

Equation 9 is rewritten by eq 10, in which the magnitudes of $k_{cs}(T)$ are regarded to be temperature-dependent as follows,

$$\frac{1}{\phi(T)} - 1 = \frac{k_{cs}(T)}{k_{ic}} = \frac{k_{cs}^o}{k_{ic}}\exp\left(-\frac{\Delta E_{cs}}{RT}\right) \tag{10}$$

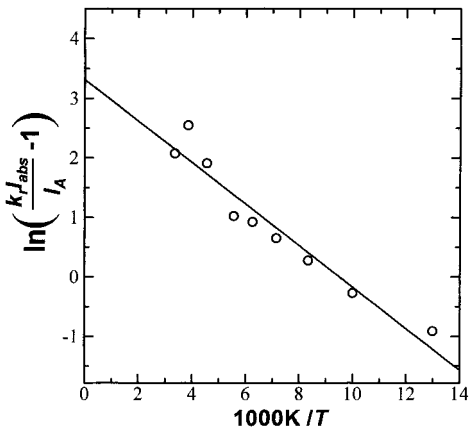

Figure 15. Plot of $\ln(k_r I_{abs}/I_S - 1)$ against the reciprocal of *RT* for the short-lived component on assuming $k_r = 7 \times 10^7$ s^{-1}. The slope of a straight line yields the extent of activation energy for the charge-separation process from the nascent exciton (0.03 eV).

where k_{cs}^o is the rate constant of charge separation at the high-temperature limit and ΔE_{cs} is the activation energy of the charge-separation process. The natural logarithm of eq 10 is rewritten by eq 11 as follows,

$$\ln\left(\frac{k_r I_{abs}}{I_s} - 1\right) = \ln\frac{k_{cs}^o}{k_{ic}} - \frac{\Delta E_{cs}}{RT} \tag{11}$$

where $1/\phi(T)$ is replaced by $(I_{abs}/I_s)\times k_r$. A linear relation in Figure 15 was obtained by assuming k_r of 7×10^8 s^{-1}, which is 14 times as large as that of a single molecule in the CH_2Cl_2 solution ($1/\tau = 2.5 \times 10^8$ s^{-1}, $\Phi_F = 0.2$, $k_r = 0.5 \times 10^8$ s^{-1}). The extent of ΔE_{cs} estimated from the linear relation (30 meV) is close to the activation energy of photocurrent in a temperature range of 200−300 K.[17]

5. Conclusion

Two crystalline forms of OTiPc, α-OTiPc-S and *β*-OTiPc-L, exhibited a wide and intense absorption band with a peak at 11 630 and 13 160 cm^{-1}, respectively. A study by means of time-correlated single photon counting revealed that fluorescence of α-OTiPc-S at 10 420 cm^{-1} is composed of the short-lived (48−64 ps) and the long-lived components (101−416 ps). The quantum yield of the fluorescent exciton of α-OTiPc-S was less than 0.1 at 298 K. The normalized initial intensity ($\phi_S \times k_r$) of the short-lived exciton was dependent on the temperature. *β*-OTiPc-L exhibited dual fluorescence at 11 900 and 10 400 cm^{-1}, of which the yield is 4.2×10^{-3} at 298 K.

The study of femtosecond time-resolved absorption spectroscopy on the chemistry of a photoexcited crystal revealed that the intrinsic exciton exhibited a difference absorption at 420−620 nm with bleaching of the ground-state absorption at 650−880 nm. The intrinsic excitons of *β*-OTiPc-L and α-OTiPc-S were replaced in 1 ps by a charge-separated pair, $^2(OTiPc)_{n-1}^+\cdots{}^2(OTiPc)^-$, with the absorption peaks at 430 and 510 nm and with a lifetime of 3 and 2 ps, respectively. A majority of the bleached ground-state absorption on the laser excitation was recovered within 10 ps, not to survive as the long-lived exciton with a lifetime of 48−64 ps. The enhanced formation of the long-lived exciton for α-OTiPc-S in a low-temperature region was ascribable to smaller conversion to $^2(OTiPc)_{n-1}^+\cdots{}^2(OTiPc)^-$ from the intrinsic exciton.

References and Notes

(1) Popovic, Z. D.; Khan, M. I.; Atherton, S. J.;. Hor, A.-M; Goodman, J. L. *J. Phys. Chem. B* **1998**, *102*, 657.

(2) Yamaguchi, S.; Sakaki, Y. *J. Phys. Chem. B* **1999**, *103*, 6835.

(3) Yamaguchi, S.; Sakaki, Y. *Chem. Phys. Lett.* **2000**, *323*, 35.

(4) Saito, T.; Sisk, W.; Kobayashi, T.; Suzuki, S.; Iwayanagi, T. *J. Phys. Chem*. **1993**, *97*, 8026.

(5) (a) Asahi, T.; Mataga, N. *J. Phys. Chem.* **1991**, *95*, 1956. (b) Asahi, T.; Ohkohchi, M.; Mataga, N. *J. Phys. Chem*. **1993**, *97*, 13132.

(6) Gould, I. R.; Noukakis, D.; Jahn, L. G.; Goodman, J. L.; Farid, S. *J. Am. Chem. Soc*. **1993**, *115*, 4405.

(7) (a) Hubig. S. M.; Kochi, J. K. *J. Phys. Chem*. **1995**, *99*, 17578. (b) Asahi, T.; Matsuo, Y.; Masuhara, H.; Kojima, H. *J. Phys. Chem. A* **1997**, *101*, 612.

(8) (a) Watanabe, K.; Asahi, T.; Fukumura, H.; Masuhara, H.; Hamano, K.; Kurata, T. *J. Phys. Chem. B* **1997**, *101*, 1510. (b) Watanabe, K.; Asahi, T. ; Fukumura, H.; Masuhara, H.; Hamano, K.; Kurata, T. *J. Phys. Chem. B* **1998**, *102*, 1182.

(9) Gulbinas, V,; Jakubenas, R.; Pakalnis, S.; Undzenas, A. *J. Chem. Phys*. **1997**, *107*, 4927.

(10) Terasaki, A.; Hosoda, M.; Wada, T.; Tada, H.; Koma, A.; Yamada, A.; Sasabe, H.; Garito, A. F.; Kobayashi, T. *J. Phys. Chem.* **1992**, *96*, 10534.

(11) Gulbinas, V.; Chachisvilis, M.; Valkunas, L.; Sundstrom, V. *J. Phys. Chem. B* **1996**, *100*, 2213.

(12) Yonehara, H.; Etori, M.; Engel, K; Tsushima, M.; Ikeda, N.; Ohno, T.; Pac, C. *Chem. Mater*. **2001**, *13*, 1015.

(13) Yao, Y.; Yonehara, H.; Pac, C. *Bull. Chem. Soc. Jpn*. **1995**, *68*, 1001.

(14) Hiller, W.; Strahle, J.; Kobel, W.; Hanack, M. Z. *Krystallogr* **1982**, *159*, 173.

(15) Enokida, T.; Hirohashi, R.; Nakamura, T. *J. Imaging Sci.* **1990,** *34*, 234.

(16) Tsushima, M.; Ikeda, N.; Nozaki, K.; Ohno, T. *J. Phys. Chem. A* **2000**, *104*, 5176.

(17) Yonehara, H.; Pac, C. To be published.

(18) Ohtani, H.; Kobayashi, T.; Ohno, T.; Kato, S.; Tanno, T.; Yamada, A. *J. Phys. Chem*. **1984**, *88*, 4431.

(19) Ohno, T.; Kato, S.; Lichtin, N. N. *Bull. Chem. Soc. Jpn*. **1982**, *55*, 2753.

(20) Ohno, T.; Kato, S. *J. Phys. Chem*. **1984**, *88*, 1670.

(21) Ogawa, K.; Yao, J.; Yonehara, H.; Pac, C. *J. Mater. Chem*. **1996**, *6*, 143.

(22) Ohno, T.; Kato, S.; Yamada, A.; Tanno T. *J. Phys. Chem*. **1983**, *87*, 775.

(23) Clack, D. W.; Yandle, J. R. *Inorg. Chem*. **1972**, *11*, 1738.

(24) Ohno, T.; Yoshimura, A.; Shioyama, H.; Mataga, N. *J. Phys. Chem.* **1987**, *91*, 4365.

(25) O'Neill, P.; Steeken, S.; Schulte-Frohlinde, D. *J. Phys. Chem.* **1975**, *79*, 2773.

(26) Rao, P. S.; Hayon, E. *J. Phys. Chem*. **1975**, *79*, 1063.

(27) Wang, X.; Kofron, W. G.; Kong, S.; Rajesh, C. S.; Modarelli, D. A.; Lim, E. C. *J. Phys. Chem. A* **2000**, *104*, 1461.

(28) Shizuka, H.; Hagiwara, H.; Fukushima, M. *J. Am. Chem. Soc*. **1985**, *107*, 7816.